Nitric Oxide-Mediated Maintenance of Redox Homeostasis Contributes to NPR1-Dependent Plant Innate Immunity Triggered by Lipopolysaccharides[1][C][W]

Aizhen Sun, Shengjun Nie, and Da Xing*

Ministry of Education Key Laboratory of Laser Life Science and Institute of Laser Life Science, College of Biophotonics, South China Normal University, Guangzhou 510631, China

The perception of lipopolysaccharides (LPS) by plant cells can lead to nitric oxide (NO) production and defense gene induction. However, the signaling cascades underlying these cellular responses have not yet been resolved. This work investigated the biosynthetic origin of NO and the role of NONEXPRESSOR OF PATHOGENESIS-RELATED GENES1 (NPR1) to gain insight into the mechanism involved in LPS-induced resistance of Arabidopsis (*Arabidopsis thaliana*). Analysis of inhibitors and mutants showed that LPS-induced NO synthesis was mainly mediated by an arginine-utilizing source of NO generation. Furthermore, LPS-induced NO caused transcript accumulation of alternative oxidase genes and increased antioxidant enzyme activity, which enhanced antioxidant capacity and modulated redox state. We also analyzed the subcellular localization of NPR1 to identify the mechanism for protein-modulated plant innate immunity triggered by LPS. LPS-activated defense responses, including callose deposition and defense-related gene expression, were found to be regulated through an NPR1-dependent pathway. In summary, a significant NO synthesis induced by LPS contributes to the LPS-induced defense responses by up-regulation of defense genes and modulation of cellular redox state. Moreover, NPR1 plays an important role in LPS-triggered plant innate immunity.

Plants have evolved inducible defense mechanisms against bacterial, fungal, and viral pathogens upon recognition of diverse bacteria-derived elicitors (Scheel, 1998). Emerging evidence suggests that pathogen-associated molecular patterns (PAMPs) are potent elicitors that play an important role in basal resistance (Jones and Dangl, 2006). PAMPs are molecular motifs conserved within a class of microbes, including lipopolysaccharides (LPS) from gram-negative bacteria, bacterial flagellin, lipoteichoic acid from gram-positive bacteria, peptidoglycans, and bacterial nucleic acids. The defense system mediated by the PAMP perception in plants is similar to the innate immunity system in animals (Cohn et al., 2001; Nürnberger et al., 2004).

Bacterial LPS, endotoxins of bacterial outer membrane, are considered to be the prototypical PAMP. LPS treatment can induce various plant defense-related responses, including the oxidative burst, nitric oxide (NO) generation, cell wall alteration, and PATHOGENESIS-RELATED (PR) gene expression (Newman et al., 2002; Braun et al., 2005; Desaki et al., 2006). In some cases, LPS do not induce direct defense responses but act to increase the speed and/or degree of induction upon subsequent pathogen inoculation (Newman et al., 2002). During defense-related responses, NO production is an important hallmark of innate immunity elicited by LPS (Melotto et al., 2006).

NO is emerging as an important multifunctional signaling molecule in plant defense (Delledonne, 2005; Corpas et al., 2011). In plants, two major enzymatic pathways are proposed for NO formation: oxidation of Arg to citrulline by a nitric oxide synthase (NOS)-like enzyme and reduction of nitrite to NO by a nitrate reductase (NR; Neill et al., 2008; Fröhlich and Durner, 2011; Gupta et al., 2011). NO is also generated from other potential sources (Bethke et al., 2004; Wimalasekera et al., 2011). A NOS-like enzyme from Arabidopsis (*Arabidopsis thaliana*), AtNOS1, has been identified based on homology to a hypothetical snail NOS (Guo et al., 2003). However, the function of AtNOS1 as a NOS has recently been questioned (Zemojtel et al., 2006); therefore, the name AtNOS1 has been changed to NITRIC OXIDE ASSOCIATED1 (AtNOA1; Crawford et al., 2006). Recent studies show that AtNOA1 actually has GTPase activity rather than NOS activity (Moreau et al., 2008; Van Ree et al., 2011). However, NOS activity as well as inhibition of NO synthesis by animal NOS inhibitors have been reported in plants (Durner et al., 1998; Corpas et al., 2009). Evidence also suggests that L-Arg-dependent NOS activity is localized in at least two subcellular compartments, peroxisomes and chloroplasts (Corpas

[1] This work was supported by the Program for Changjiang Scholars and Innovative Research Team in University (grant no. IRT0829), the Key Program of National Natural Science Foundation of China-Guangdong Joint Funds of China (grant no. U0931005), and the National High Technology Research and Development Program of China, 863 Program (grant no. 2007AA10Z204).

* Corresponding author; e-mail xingda@scnu.edu.cn.

The author responsible for distribution of materials integral to the findings presented in this article in accordance with the policy described in the Instructions for Authors (www.plantphysiol.org) is: Da Xing (xingda@scnu.edu.cn).

[C] Some figures in this article are displayed in color online but in black and white in the print edition.

[W] The online version of this article contains Web-only data.

www.plantphysiol.org/cgi/doi/10.1104/pp.112.201798

et al., 2004; Jasid et al., 2006). Oxidative stress-induced redox imbalance is often triggered by pathogen attack. However, plants have antioxidant systems, including enzymatic antioxidants, such as superoxide dismutase (SOD), catalase (CAT), and peroxidase (POD), as well as nonenzymatic antioxidants, such as glutathione, ascorbic acid, and tocopherols, which help restore the redox homeostasis and alleviate oxidative damage (Mittler, 2002; Apel and Hirt, 2004). Alternative oxidase (AOX) activation plays a role in detoxification of the harmful effect of reactive oxygen species (ROS) and in the maintenance of cellular redox homeostasis under adverse stresses (Moore et al., 2002). Fu et al. (2010) demonstrated the cross talk of mitochondrial AOX and NO in the induction of antiviral defense response against tobacco mosaic virus infection. These findings indicate that NO is possibly connected with antioxidant mechanisms that underlie elicitor-induced cellular responses.

NONEXPRESSOR OF PATHOGENESIS-RELATED GENES1 (NPR1), a key regulator of systemic acquired resistance (SAR), is essential for salicylic acid (SA) signal transduction (Rockel et al., 2002). In an uninduced state, NPR1 is present as an inactive oligomer formed through intermolecular disulfide bonds. During SA induction, NPR1 is reduced to an active monomer that can translocate from the cytosol to the nucleus, which leads to defense gene activation (Mou et al., 2003). NPR1 plays important roles in activating defense genes and mediating plant defense responses (Zhang et al., 1999). In addition, during pathogen or SA induction, NPR1 regulates the high transcript accumulation of callose synthase genes *CalS1* and *CalS12* in the formation of callose (Dong et al., 2008), which is related to defenses against fungal and oomycete pathogens. LPS are known to activate the *PR* gene and to promote innate immune responses in plants. Considerable efforts have been made to evaluate the molecular mechanisms and the associated signal transduction cascades of LPS during the activation of defense responses. LPS from various sources can induce defense responses in pepper (*Capsicum annuum*) without triggering the oxidative burst and SA synthesis (Newman et al., 2002). In contrast, Zeidler et al. (2004) showed that LPS-treated Arabidopsis could cause NO generation, which plays a significant role in defense gene activation. NO is a redox regulator of the NPR1/TGA1 (for TGACG-sequence-specific DNA-binding protein) system that promotes the nuclear translocation of NPR1 (Lindermayr et al., 2010). However, the role of NPR1 in the LPS-induced defense responses in Arabidopsis is undefined.

In this study, we investigated the signaling mechanism of NO during LPS treatment and demonstrated the important role of NPR1 in LPS-induced innate immunity. Pharmacological and cellular microscopic evidence obtained in vivo indicated that LPS trigger an Arg-utilizing source of NO generation. The evidence likewise demonstrated the role of NO in LPS-induced defense responses by up-regulation of defense genes and modulation of the cellular redox state. We further studied the role of NPR1 in LPS-induced plant defense responses including *PR1* induction and callose deposition. Our results demonstrate that NO-mediated maintenance of redox homeostasis contributes to NPR1-dependent defense response triggered by LPS.

RESULTS

LPS Protect Arabidopsis from Pathogen Infection

LPS from gram-negative bacteria stimulate a series of defense-associated plant responses and strongly enhance the plant response to subsequent bacterial infection (Dow et al., 2000). When Arabidopsis plants were inoculated with *Pseudomonas syringae* pv *maculicola* (*Pma*) DG3 (virulent), the wild-type plant leaves without LPS treatment turned light yellow and finally wilted and died (Fig. 1A); whereas plants pretreated with 100 μg mL^{-1} LPS showed no visible symptoms at 3 d post inoculation (dpi), although minute yellow disease lesions were observed at 5 dpi. The *npr1* mutant plants showed more developed chlorotic lesions compared with wild-type plants, and LPS-treated *npr1* plants showed no significant improvement on disease progression both at 3 and 5 dpi. In addition, the numbers of bacteria were significantly reduced by LPS treatment in wild-type plants but not in *npr1* plants (Fig. 1B). This finding correlated with the disease symptoms shown in Figure 1A. For the pathogen-growth assays in Figure 1B, the *npr1* Arabidopsis plants were more susceptible than wild-type plants and showed obvious lesions at 5 dpi. Such damaged leaves resulted in nutrition loss and limited bacterial growth rate. Therefore, the bacterial numbers in *npr1* plants were nearly maximal at 3 dpi (Fig. 1B).

Significant Role of NOS-Like Enzyme in Mediating LPS-Induced NO Synthesis in Protoplasts

NR and NOS are two key enzymes responsible for plant NO biosynthesis. It seems that plant NOS is not a canonical animal NOS, but it uses the same substrate and cofactors as the animal NOS. Therefore, pharmacological analyses with mammalian NOS inhibitors are often used to study the physiological mechanism of plant NO production. However, the effects of mammalian NOS inhibitors in plants are somewhat difficult to interpret, because the molecular targets and specificity of these compounds are unknown. In this experiment, we combined pharmacological and genetic approaches to investigate the potential source of NO using a mesophyll protoplast system. The freshly isolated Arabidopsis mesophyll protoplasts are similar to those in intact tissues and plants in physiological and cell-autonomous responses (Tena et al., 2001). LPS-induced NO accumulation could be detected after approximately 80 min and leveled off at about 150 min (Supplemental Fig. S1). LPS application resulted in a significant increase of 3-amino,4-aminomethyl-2′,7′-

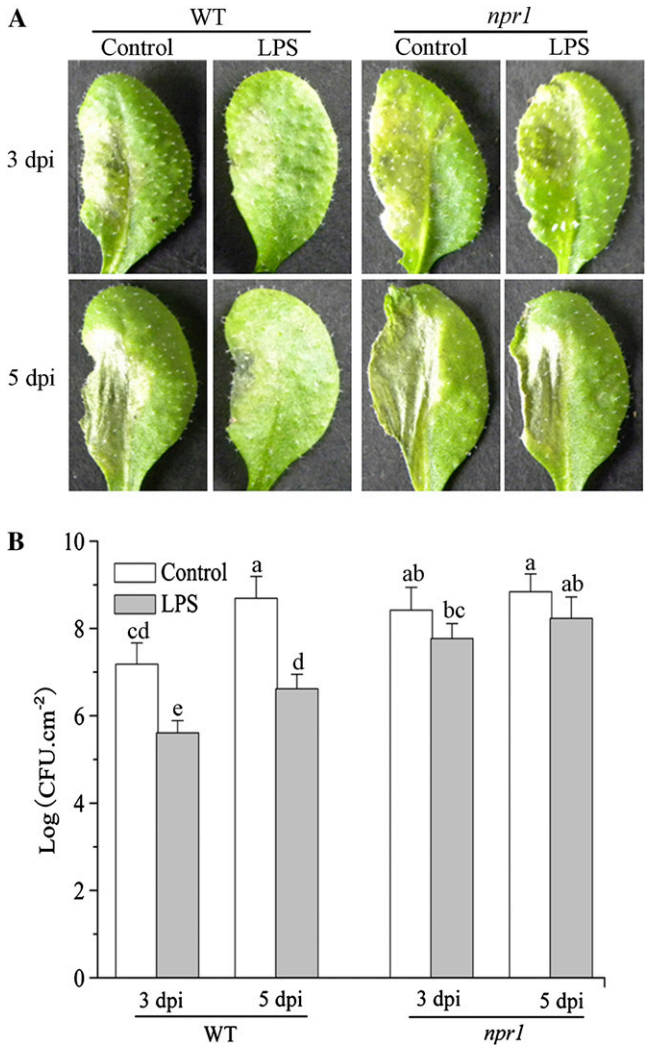

Figure 1. Effect of LPS application on disease progression in leaves of wild-type (WT) and *npr1* plants. A, After spraying with 250 μM $MgCl_2$ and 100 μM $CaCl_2$ (control solution) or LPS (100 μg mL^{-1} in 250 μM $MgCl_2$ and 100 μM $CaCl_2$) solution for 24 h, wild-type Arabidopsis and *npr1* mutant plants were inoculated with pathogen *Pma* DG3 (OD_{600} = 0.01 in 10 mM $MgCl_2$). Leaves were infected on their left halves, and samples were collected at 3 and 5 dpi. B, Bacterial growth quantification of *Pma* DG3-inoculated (OD_{600} = 0.0001) leaves after spraying with control solution or 100 μg mL^{-1} LPS. Samples were collected at 3 and 5 dpi for assay. Each value is the mean ± SE of three replicates. Different letters indicate statistically significant differences between treatments (Duncan's multiple range test: $P < 0.05$). CFU, Colony-forming units. [See online article for color version of this figure.]

difluorescein (DAF-FM) fluorescence, which could not be inhibited by the NR inhibitor sodium tungstate. However, the increases were markedly decreased by incubating the protoplasts together with the mammalian NOS inhibitors N^{ω}-nitro-L-arginine (L-NNA; 300 μM), N^{G}-nitro-L-arginine-methyl ester (L-NAME; 300 μM), or the NO scavenger 2-(4-carboxyphenyl)-4,4,5,5-tetramethylimidazoline-1-oxyl-3-oxide (cPTIO; 300 μM; Fig. 2, A and C). Furthermore, we tested the NO level in mutant *nia1nia2* Arabidopsis that exhibited null NR activity (Zhao et al., 2009), the *Atnoa1* mutant, the *gsnor1-3* plant (also named *hot5-2*), which is a loss-of-function mutation in Arabidopsis *S*-NITROSOGLUTATHIONE REDUCTASE1 (AtGSNOR1; Feechan et al., 2005), and the *cue1* mutant (also known as *nox1*) with elevated L-Arg levels. In contrast to the wild-type plant, *nia1-nia2*, and *Atnoa1* Arabidopsis, in which no significant DAF-FM fluorescence was observed, *gsnor1-3* and *cue1* mutant protoplasts showed increased endogenous NO levels under normal conditions. Protoplasts of *gsnor1-3* and *cue1* exhibited significantly high levels of DAF-FM signals under LPS induction (Fig. 2, B and C). Although the basal NO level in *Atnoa1* and *nia1nia2* plants was lower than that in wild-type plants, the DAF-FM fluorescence levels of protoplasts from both these mutants were also elevated under LPS treatment. It has been suggested that DAF does not react directly with the NO free radical but does so with NO-derived species (such as N_2O_3; Mur et al., 2011). To confirm that the changes in fluorescence were caused by NO itself, electron paramagnetic resonance (EPR) analysis was also used. The presented data also demonstrated NO production after LPS treatment (Fig. 2D). In addition, an increase in NOS-like enzyme activity was detected during LPS induction, and these increases were dramatically inhibited by L-NNA and L-NAME (Fig. 2E). Moreover, under LPS treatment, we did not observe any increased NR activity in both wild-type and *nia1nia2* plants. On the contrary, a slight inhibition of NR activity was seen in wild-type plants (Fig. 2F). The results demonstrate that the NOS-like enzyme possibly plays a key role in LPS-elicited NO generation.

LPS-Activated Defense Responses Are Dependent on NPR1

The transgenic *PR1*:*GUS* reporter plants were used to detect the *PR1* gene expression (Gust et al., 2007), which marks the SA-dependent gene expression. As shown in Figure 3A, when the seedlings were grown on Murashige and Skoog (MS) medium with LPS, a strong *PR1*:*GUS* expression was induced; *PR1*:*GUS* in these transgenic seedlings was present primarily in the cotyledons and in the older leaves, but it was absent in the roots. The Arabidopsis NPR1 protein plays an essential role in SA-mediated SAR (Kinkema et al., 2000). To test whether LPS-activated *PR1* expression acts through an NPR1-dependent signaling pathway, the effect of LPS on *PR1* activation in wild-type and *npr1* mutant plants was investigated. A transient increase in *PR1* transcripts was detected at 6 h after LPS application in wild-type plants and showed high accumulation at 12 h. However, LPS treatment did not promote increased *PR1* transcripts in the *npr1* plants (Fig. 3B).

We further analyzed callose deposition and the expression of *CalS1* and *CalS12* genes to investigate the role of NPR1 on these LPS-induced responses. After 24 h of LPS treatment, callose deposition was observed in wild-type plants but not in *npr1* plants (Fig. 3, C–E).

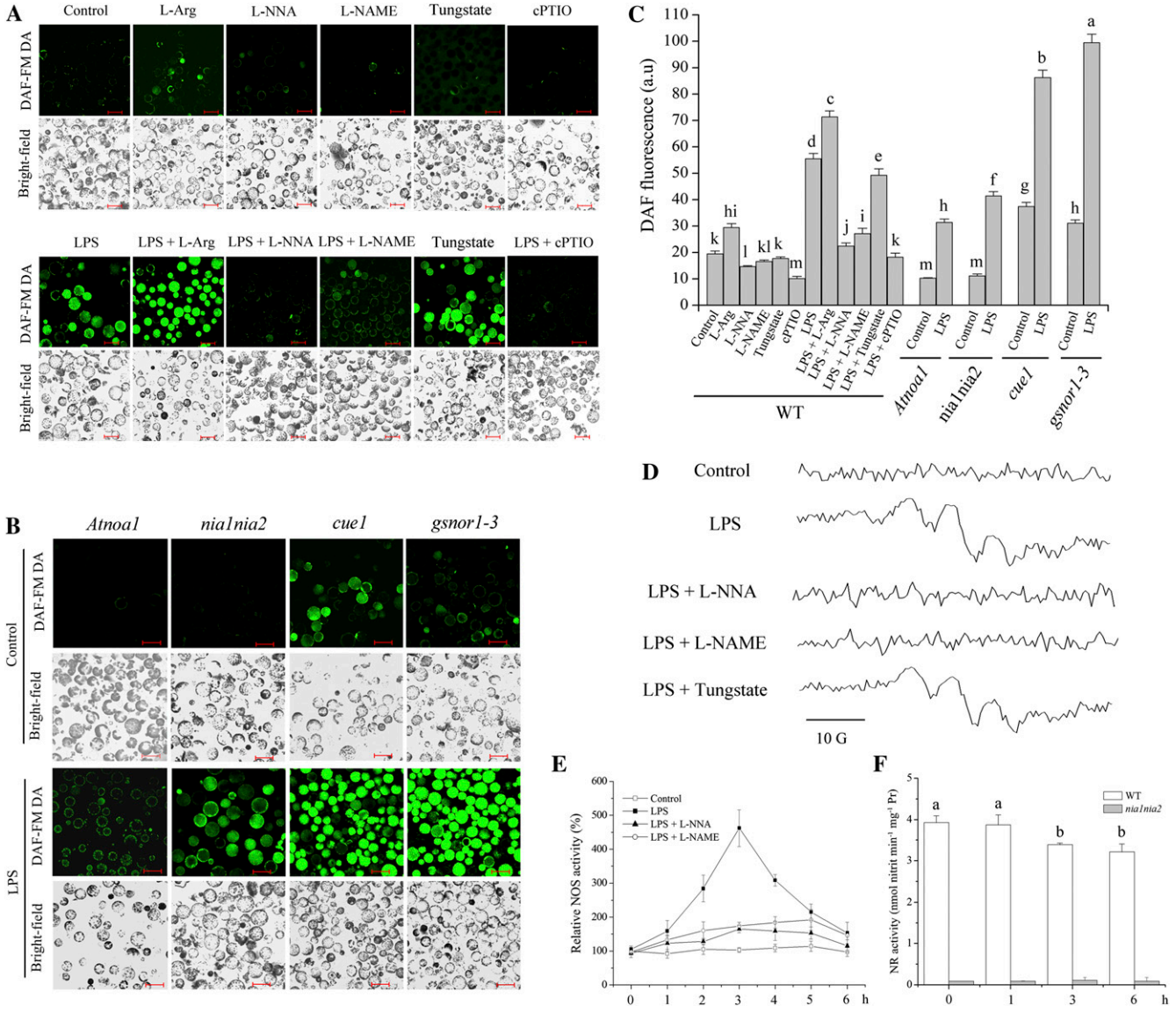

Figure 2. LPS-elicited Arg-utilizing source of NO generation. A, Effects of mammalian NOS inhibitors and NO scavenger on NO level by LPS induction. Protoplasts prepared from wild-type plants were loaded with DAF-FM DA for 20 min prior to different treatments for 2 h. For each treatment, fluorescence and bright-field images are shown. B, Confocal images of DAF-FM fluorescence in protoplasts from *Atnoa1*, *nia1nia2*, *cue1*, and *gsnor1-3* plants treated with control solution or 100 μg mL^{-1} LPS for 2 h. Bars = 50 μm. C, Quantitative analysis of NO-related DAF-FM fluorescence by a fluorescence spectrometer under various treatments for 2 h as shown in A and B. WT, Wild type. D, NO production was examined by EPR analysis. E, Effect of LPS and mammalian NOS inhibitors on NOS-like enzyme activity. F, Effect of LPS on NR activity of wild-type and *nia1nia2* plants. Pr, Protein. Data are means ± SE of three experiments. Different letters indicate statistically significant differences between treatments (Duncan's multiple range test: $P < 0.05$). [See online article for color version of this figure.]

Analysis of *CalS1* and *CalS12* gene expression by reverse transcription (RT)-PCR revealed that, after 12 h of LPS treatment, the *CalS1* and *CalS12* transcripts were significantly increased in wild-type plants (Fig. 3, F and G), whereas no significant differences in the amount of RT-PCR products were found in the *npr1* mutant plants with and without LPS treatment (Fig. 3, F and G). In fully grown Arabidopsis, LPS could also induce *PR1* gene expression and callose deposition (Supplemental Fig. S2). These data imply that LPS induction leads to direct *PR1* transcription and callose deposition, which are related to an NPR1-dependent signaling pathway.

LPS Treatment Leads to a Nuclear Localization of NPR1

To test the hypothesis that LPS might affect the subcellular localization of NPR1, we analyzed the distribution of NPR1-GFP during LPS induction. Cytosolic fluorescence in a protoplast system is difficult

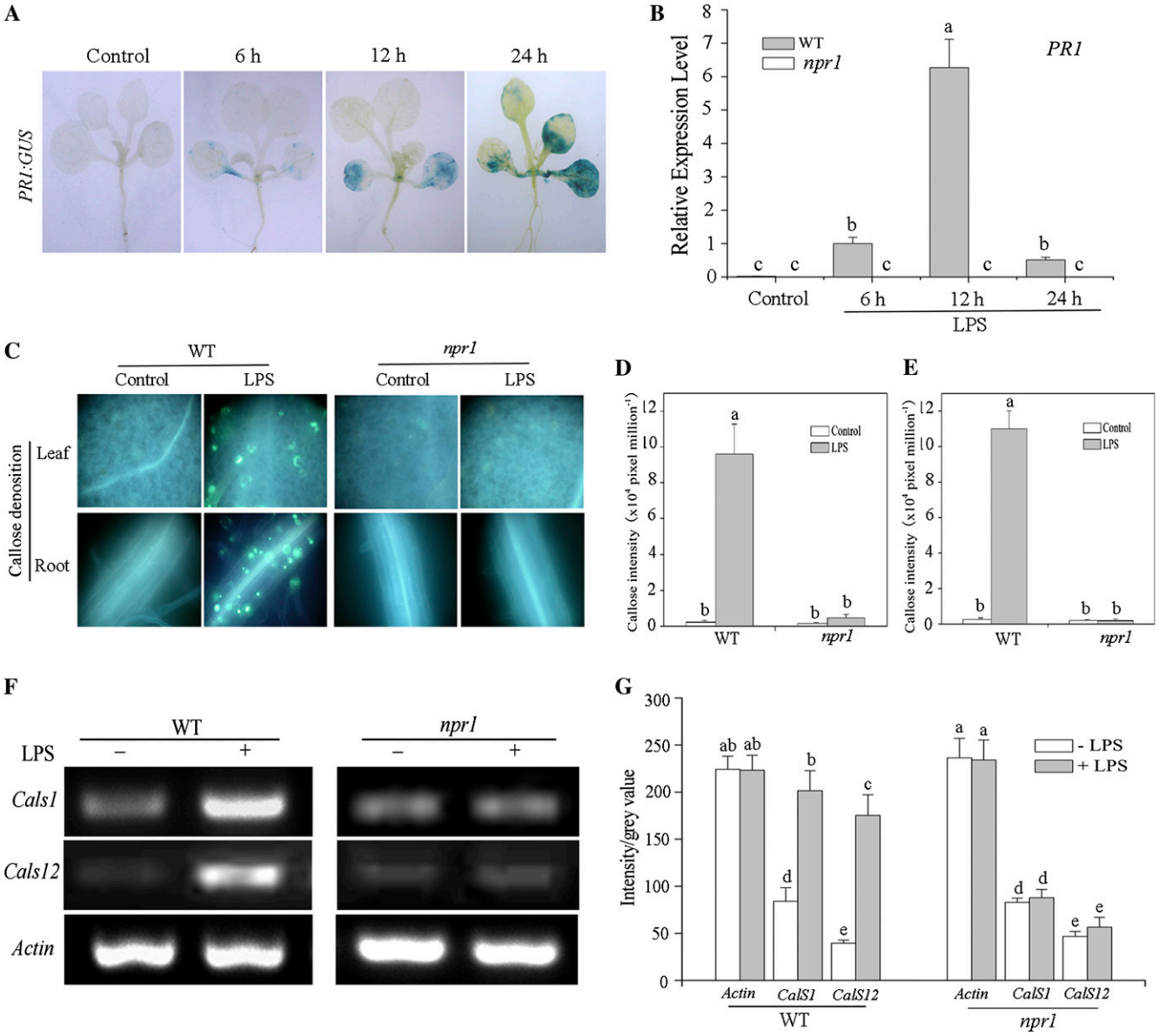

Figure 3. Induction of *PR1* gene expression and callose deposition in Arabidopsis by LPS. A, Approximately 10-d-old transgenic *PR1*:*GUS* seedlings grown on MS medium were then transferred to 24-well plates containing 400 μL of liquid MS medium without 100 μg mL^{-1} LPS (control) for 12 h or with 100 μg mL^{-1} LPS for 6, 12, or 24 h and collected for histochemical GUS staining. Each experiment was performed with eight plants and repeated twice with similar results. B, Quantitative RT-PCR data showing the expression of the *PR1* gene in wild-type (WT) and *npr1* Arabidopsis. Total RNA was extracted from the leaves of Arabidopsis after spraying with control solution at 12 h post treatment or 100 μg mL^{-1} LPS at 0, 6, 12, and 24 h post treatment. Arabidopsis *ACTIN2* was used as an internal control. Expression levels for each treatment were normalized to a LPS-treated (6 h) wild-type plant. Values represent means ± SE of three independent experiments. C, Callose-staining imaging of leaves and roots from LPS-treated plants. D and E, Callose deposition in leaves (D) and roots (E) was quantified by determining the number of pixels (corresponding to LPS-induced callose) per million pixels in digital photographs. Data are means ± SE of three experiments. F, Induction of *CalS1* and *CalS12* genes in wild-type and *npr1* mutant Arabidopsis by LPS treatment. Total RNA was extracted from leaves treated with control solution (−) or 100 μg mL^{-1} LPS (+) for 12 h. *ACTIN2* was used as an internal control. The experiment was performed three times with similar results. G, Quantitative analysis of *CalS1* and *CalS12* genes shown in F with ImageJ software. Three gel photographs were taken for quantitative analysis, and values represent means ± SE. Different letters indicate statistically significant differences between treatments (Duncan's multiple range test: $P < 0.05$). [See online article for color version of this figure.]

to detect because the fusion protein in larger cells is too diffuse, as pointed out by Kinkema et al. (2000). Thus, guard cells, in which the amount of NO could also be induced by LPS (Supplemental Fig. S3), were used in this experiment for analysis. As shown in Figure 4, while in the treatment with control solution, NPR1-GFP fluorescence mainly occurred in the cytoplasm, with a small amount occurring in the guard cell nuclei. However, strong NPR1-GFP fluorescence localized predominantly to the guard cell nuclei when the seedlings were treated with LPS. NO scavenging with cPTIO or inhibitors of the mammalian NOS (L-NNA, L-NAME) prevented the translocation into the nucleus. Unless otherwise mentioned, the concentration of cPTIO used in this and following experiments was 1 mM (Supplemental Fig. S4). 2-Aminoindan-2-phosphonic acid (AIP), an inhibitor of Phe ammonia lyase, also partially inhibited LPS-induced nuclear localization of NPR1. Moreover, the addition of the NO scavenger cPTIO, mammalian NOS inhibitors, or AIP alone did not induce the nuclear translocation of NPR1-GFP. A nuclear localization of NPR1 was also detected in protoplasts during LPS treatment (Supplemental Fig. S5). These results suggest that LPS treatment resulted in a nuclear localization of NPR1, for which a NO-modulated mechanism is responsible.

Involvement of NO in the Induction of *AOX* Gene Expression and the Up-Regulation of Antioxidant Enzyme Activity

As early as 3 h, the *AOX1a* and *AOX1b* transcripts significantly increased upon LPS induction. Genes were apparently expressed after 6 and 9 h of treatment, albeit to a lesser extent than that at 3 h (Fig. 5, A and B). However, *AOX1c* and *AOX1d* only showed slight accumulation, and the expression of *AOX2* was almost not changed (Fig. 5, C–E). Furthermore, we also evaluated *AOX* gene expression with the NO scavenger cPTIO and inhibitors of mammalian NOS to determine the specificity of NO signal. The evidence that LPS plus cPTIO, L-NNA, or L-NAME markedly reduced *AOX1a* and *AOX1b* induction supported the conclusion that NO was positively correlated with the LPS induction of *AOX* genes. In addition, compared with that in wild-type Arabidopsis, *AOX1a* and *AOX1b* transcript accumulations were reduced in the *npr1* mutant (Fig. 5F).

Enzymatic and nonenzymatic antioxidants play important roles in ROS scavenging and thereby influence the cellular ROS level. The activities of three significant antioxidant enzymes (SOD, POD, and CAT) were assessed in the LPS-treated leaves. As shown in Figure 6, significant increases of SOD, POD, and CAT activities occurred at 6 h in wild-type Arabidopsis. The *npr1* mutant showed lower enzyme activities than wild-type plants (Fig. 6D). The LPS-induced increases in antioxidant enzyme activities (SOD, POD, and CAT) were decreased by the NO scavenger cPTIO and mammalian NOS inhibitors (Fig. 6, A–C). These results point to the involvement of NO in the LPS-induced up-regulation of antioxidant enzyme activities.

NO-Mediated Processes in the Regulation of Cell Redox Status

Pathogen attack triggers ROS production, especially hydrogen peroxide (H_2O_2), which could result in oxidative

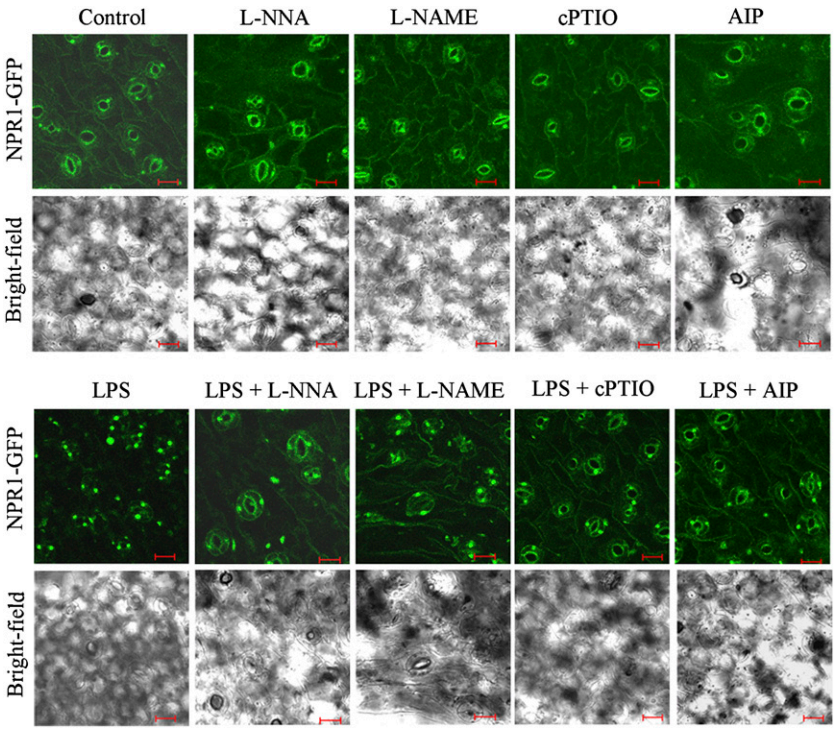

Figure 4. LPS induction results in nuclear localization of NPR1. Approximately 10-d-old transgenic *35S:NPR1-GFP* seedlings grown on MS medium were then transferred to 24-well plates containing control solution, 300 μM L-NNA, 300 μM L-NAME, 1 mM cPTIO, 50 μM AIP, 100 μg mL^{-1} LPS, 100 μg mL^{-1} LPS + 300 μM L-NNA, 100 μg mL^{-1} LPS + 300 μM L-NAME, 100 μg mL^{-1} LPS + 1 mM cPTIO, or 100 μg mL^{-1} LPS + 50 μM AIP for 12 h. GFP fluorescence in guard cells was observed with a laser confocal scanning microscope. Results shown are representative. Bars = 20 μm. [See online article for color version of this figure.]

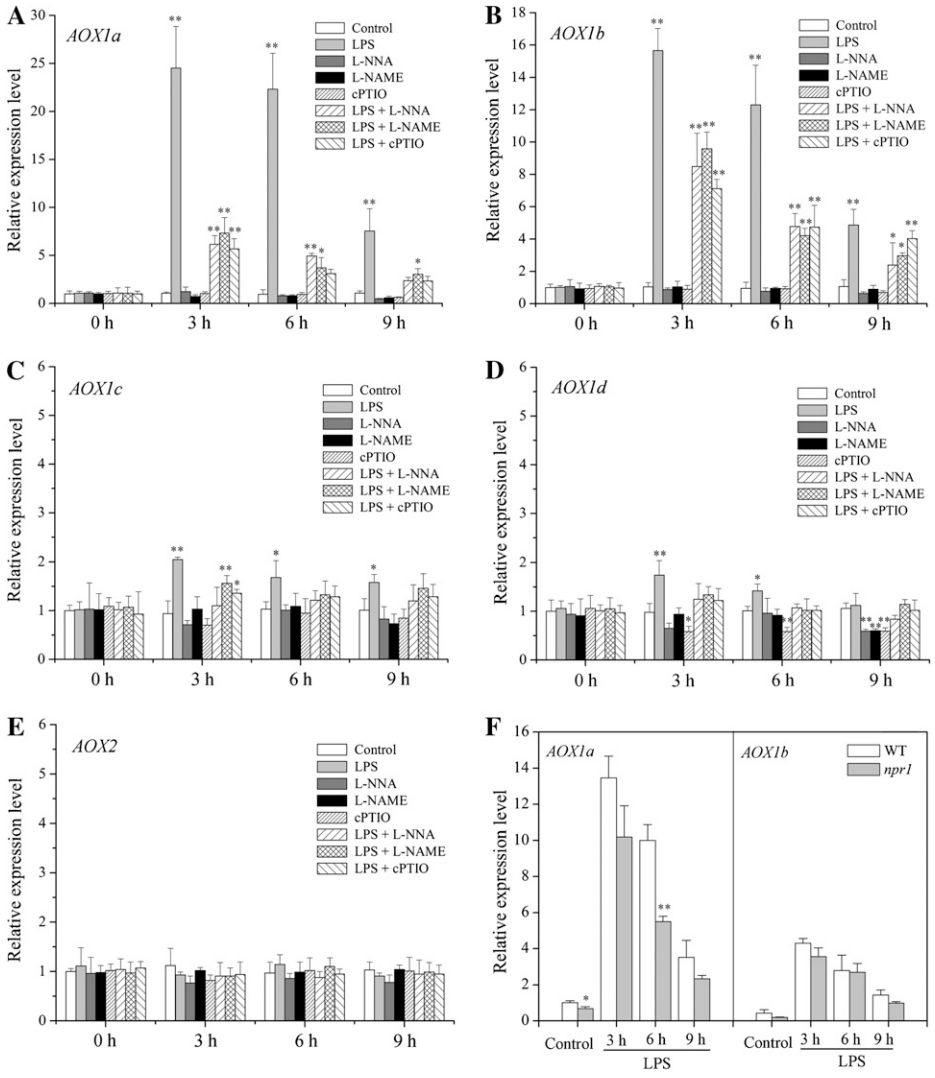

Figure 5. A to E, Transcript levels of *AOX1a* (A), *AOX1b* (B), *AOX1c* (C), *AOX1d* (D), and *AOX2* (E) in wild-type Arabidopsis plants under LPS treatment. Total RNA was extracted from the leaves of full-grown Arabidopsis after spraying with control solution, 300 μM L-NNA, 300 μM L-NAME, 1 mM cPTIO, 100 μg mL^{-1} LPS, 100 μg mL^{-1} LPS + 300 μM L-NNA, 100 μg mL^{-1} LPS + 300 μM L-NAME, or 100 μg mL^{-1} LPS + 1 mM cPTIO at 3, 6, and 9 h post treatment. Arabidopsis *ACTIN2* was used as an internal control. Asterisks indicate significant differences from the control (Duncan's multiple range test: $*P < 0.05$, $**P < 0.01$). F, Transcript levels of *AOX1a* and *AOX1b* in wild-type and *npr1* Arabidopsis. Asterisks indicate significant differences between the wild type and the mutant (Student's paired *t* test: $*P < 0.05$, $**P < 0.01$). Expression levels for each gene were normalized to control treatment (0 h) of the wild-type plant. Values represent means ± SE of three independent experiments.

damage and impairment of cellular functions. AOX and enzymatic antioxidants play significant roles in ROS scavenging and thus influence the cellular redox state. The oxidized reduction-oxidation sensitive (ro)GFP in transgenic Arabidopsis that expressed mitochondrial (mit)-roGFP1 was measured to evaluate the redox state following inhibitor treatment. LPS pretreatment decreased the pathogen *Pma* DG3-induced mit-roGFP1 oxidation as well as H_2O_2 production, whereas this effect was reversed by the AOX inhibitor salicylhydroxamic acid (SHAM), inhibitors of the mammalian NOS (L-NNA, L-NAME), and the NO scavenger cPTIO (Fig. 7, A–C; Supplemental Fig. S6).

Furthermore, we determined the levels of reduced glutathione (GSH) and oxidized glutathione (GSSG), which is an important antioxidant buffer system, to get more information on overall cellular redox states. During the pathogen infection, GSH-to-GSSG ratios decreased, reflecting an increasing oxidative stress (Fig. 7E). Total antioxidant capacity, as an indicator of the intracellular redox state, was also decreased after the pathogen challenge (Fig. 7F). LPS pretreatment could enhance GSH-to-GSSG ratio and antioxidant capacity, however, which were drastically reduced with inhibitor treatments (Fig. 7, E and F).

NO Is Responsible for LPS-Induced Plant Defense Responses

The effects of mammalian NOS inhibitors and NO scavenger on callose deposition and *PR1* gene expression were studied to investigate the role of NO production in LPS-induced plant innate immunity. Callose deposition and *PR1* gene expression by LPS induction were partially reduced by L-NNA, L-NAME, and cPTIO after treatment for 12 h (Fig. 8, A–C). LPS treatment inhibited bacterial growth, and application of 200 μM sodium nitroprusside (SNP) could also reduce the bacterial number; however, L-NNA, L-NAME, and cPTIO infiltration impaired the effect of LPS

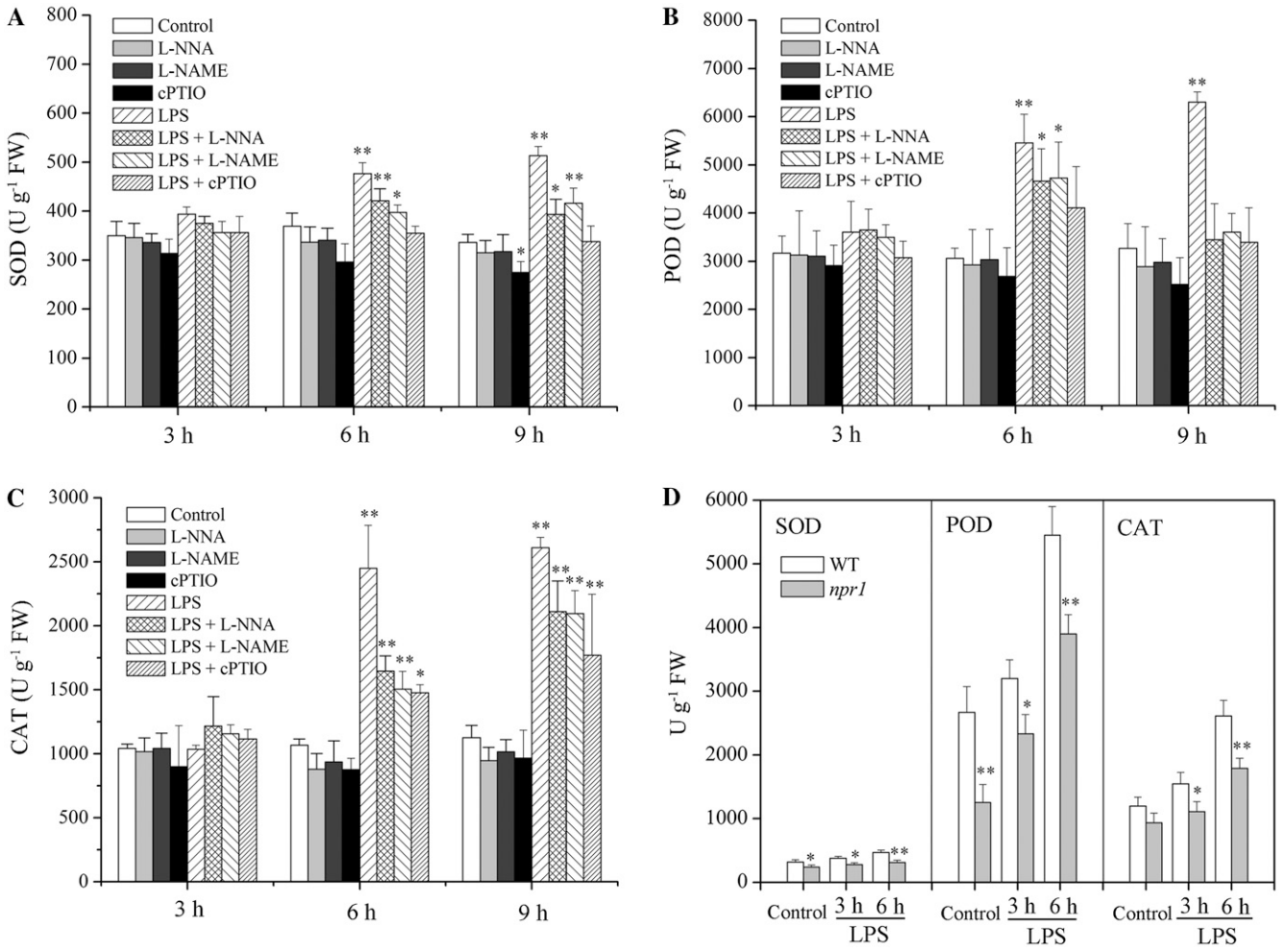

Figure 6. A to C, Activities of antioxidant enzymes during LPS and NO scavenger treatment. Leaves were treated with control solution, 300 μM L-NNA, 300 μM L-NAME, 1 mM cPTIO, 100 μg mL^{-1} LPS, 100 μg mL^{-1} LPS + 300 μM L-NNA, 100 μg mL^{-1} LPS + 300 μM L-NAME, or 100 μg mL^{-1} LPS + 1 mM cPTIO for 3, 6, and 9 h and then collected for determination of SOD (A), POD (B), and CAT (C) activities. Asterisks indicate significant differences from the control (Duncan's multiple range test: $*P < 0.05$, $**P < 0.01$). D, Activities of antioxidant enzymes in wild-type (WT) and *npr1* Arabidopsis. Asterisks indicate significant differences between the wild-type and the mutant (Student's paired *t* test: $*P < 0.05$, $**P < 0.01$). FW, Fresh weight; U, units. Data are means ± SE of at least three independent experiments.

treatment (Fig. 8D). Therefore, NO plays a crucial role in LPS-induced defense responses as an early signal molecule.

DISCUSSION

The experimental evidence supports that LPS, as a plant defense activator, can lead to NO production and play a key role in plant disease resistance (Delledonne et al., 1998; Melotto et al., 2006). However, the biosynthetic origin of NO and the signaling mechanisms underlying these cellular responses are not fully resolved. Our findings demonstrated that LPS treatment protected Arabidopsis from bacterial infection (Fig. 1). Enhanced disease perturbation confirms the alternative role of LPS as a PAMP elicitor to trigger defense responses. *PR1* gene expression and callose deposition are indicators of defense-related responses (van Loon and van Strein, 1999; Ton and Mauch-Mani, 2004). Some biological agents and synthetic compounds cannot induce *PR1* expression and callose deposition per se until pathogen infection; these induced reactions are based on primed accumulation (Ton and Mauch-Mani, 2004; van Hulten et al., 2006; Ahn et al., 2007). However, a number of elicitors can induce direct callose accumulation (Gómez-Gómez et al., 1999; Galletti et al., 2008; Millet et al., 2010). In this study, we found that LPS, as a typical PAMP, could directly induce such defense-related responses (Fig. 3). Therefore, the cellular defense responses involved in induced resistance are either activated directly or primed for augmented

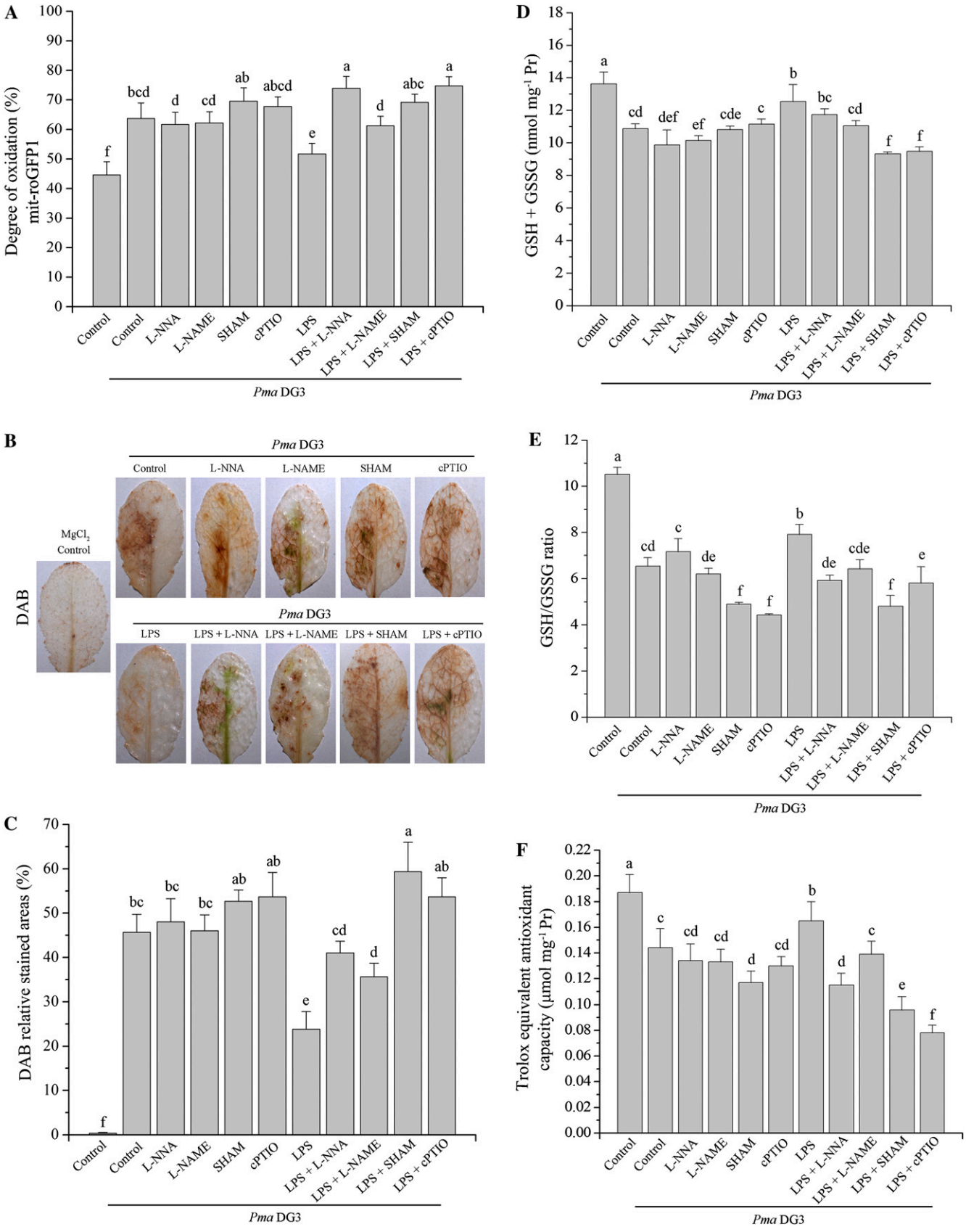

Figure 7. Changes in redox state and antioxidant capacity during various treatments. A, After spraying with control solution, 300 μM L-NNA, 300 μM L-NAME, 200 μM SHAM, 1 mM cPTIO, 100 μg mL^{-1} LPS, 100 μg mL^{-1} LPS + 300 μM L-NNA, 100 μg mL^{-1} LPS + 300 μM L-NAME, 100 μg mL^{-1} LPS + 200 μM SHAM, or 100 μg mL^{-1} LPS + 1 mM cPTIO for 12 h, leaves of

expression upon pathogen attack. Although directly activated and primed resistances seem to share several common features, including callose deposition and defense-related gene expression, the differences suggest that different mechanisms exist. Determining the corresponding mechanisms is a challenge and will be the focus of future research. LPS-induced *PR1* accumulation was observed in leaves but not in roots, whereas the LPS-induced callose accumulated significantly both in leaves and roots of wild-type Arabidopsis (Fig. 3, A and C), implying that different physiological and developmental signals are possibly involved in different tissues in response to LPS. The *PR1*:*GUS* expression and callose deposition in fully grown LPS-treated Arabidopsis were much weaker than those in Arabidopsis seedlings grown in liquid MS medium with LPS (Supplemental Fig. S2). One possible explanation is that LPS is more readily taken up by seedlings than by fully grown plants. Taken together, our findings indicate that *PR1* transcription and callose deposition that are directly induced by LPS constitute plant innate immunity, which protects Arabidopsis against pathogen infection.

NO-Mediated Maintenance of Redox Homeostasis Contributes to LPS-Induced Plant Resistance Responses

Two key enzyme pathways are responsible for NO synthesis in plants: reduction of nitrite to NO by NR and oxidation of Arg to citrulline by NOS (Besson-Bard et al., 2008; Neill et al., 2008). Although considerable efforts need to be made to identify the plant NOS activity, a summary of the L-Arg-dependent NOS activities detected in tissues of different plant species supports the existence of NOS activity in plants (Corpas et al., 2009). In this study, the endogenous NO level in wild-type protoplasts was markedly decreased after the addition of inhibitors of the mammalian NOS but not after the addition of sodium tungstate, an NR inhibitor (Fig. 2). Although pharmacological analyses with mammalian NOS inhibitors have been used to explore the mechanisms of LPS-induced NO production in Arabidopsis, it should be noted that significant questions remain concerning the specificity and targets of these compounds in plants. Besides NOS, mammalian NOS inhibitors could also affect the activities of other L-Arg-metabolizing enzymes and have been proposed to interact with other substances (Peterson et al., 1992; Besson-Bard et al., 2008). Recent evidence also suggests that L-NAME could inhibit NR activity (Rasul et al., 2012). Therefore, we should also not rule out the possibility that the effects of mammalian NOS inhibitors could be complex.

Furthermore, NR-null mutant *nia1nia2* protoplasts also generated NO induced by LPS (Fig. 2). A slight inhibition of NR activity was also seen in wild-type plants by LPS treatment (Fig. 2F), while the transcript levels of *NIA1* and *NIA2* did not decrease (Supplemental Fig. S7). It has been proposed that posttranslational regulation of NR takes place in response to various treatments (Lillo et al., 2004). We did not show evidence whether NR was modulated by a posttranslational mechanism or how the NR activity was regulated. Further studies to elucidate the mechanism are warranted. Moreover, the addition of L-Arg promoted NO generation, and the *cue1* mutant, which accumulates L-Arg, also showed high NO levels during LPS treatment. These observations provide further support for the hypothesis that the L-Arg-dependent NOS-like enzyme is likely responsible for the biosynthetic mechanism involved in LPS-induced NO because L-Arg is the NOS substrate for generating NO. GSNOR, which reduces *S*-nitrosoglutathione to GSSG and NH_3, plays critical roles in modulating cellular NO status (Lee et al., 2008). The higher NO content in *gsnor1-3* mutant protoplasts than in the wild type under LPS treatment (Fig. 2) suggests that GSNOR activity is involved in the regulation of NO contents in our conditions.

Delledonne et al. (1998) reported that NO can potentiate hypersensitive cell death concomitant with the ROS burst during inoculation with an avirulent pathogen, but less ROS were produced together with NO in response to a virulent strain. In our study here, NO alleviated mit-roGFP1 oxidation and decreased 3,3′-diaminobenzidine (DAB) staining during LPS induction (Fig. 7). These results indicate that different mechanisms underlie NO-modulated resistance responses between virulent and avirulent pathogen attacks. Palmieri et al. (2010) provided evidence for the cross talk between NO and mitochondria in activating the stress-related response in plants. The study of Fu et al. (2010) highlighted a role for transcriptional activation of mitochondrial AOX in triggering systemic basal defenses against *Tobacco mosaic virus*. The data presented here suggested the involvement of NO in mediating the expression of the *AOX* gene and the upregulation of antioxidant enzyme activities. Measurement

Figure 7. (*Continued.*)
transgenic mit-roGFP1 Arabidopsis were inoculated with Pma DG3 (OD_{600} = 0.01) and then collected at 12 h for measurement of mit-roGFP1 oxidation. B to F, Pma DG3-inoculated leaves of wild-type plants under various treatments were collected at 24 h for DAB staining indicating H_2O_2 generation (B) and quantitative analysis of DAB-stained areas (C) and were collected at 12 h for determination of glutathione levels (D), the ratios of GSH to GSSG (E), and total antioxidant capacity (F). Pr, Protein. Data are means ± SE of at least three independent experiments. Different letters indicate statistically significant differences between treatments (Duncan's multiple range test: $P < 0.05$). [See online article for color version of this figure.]

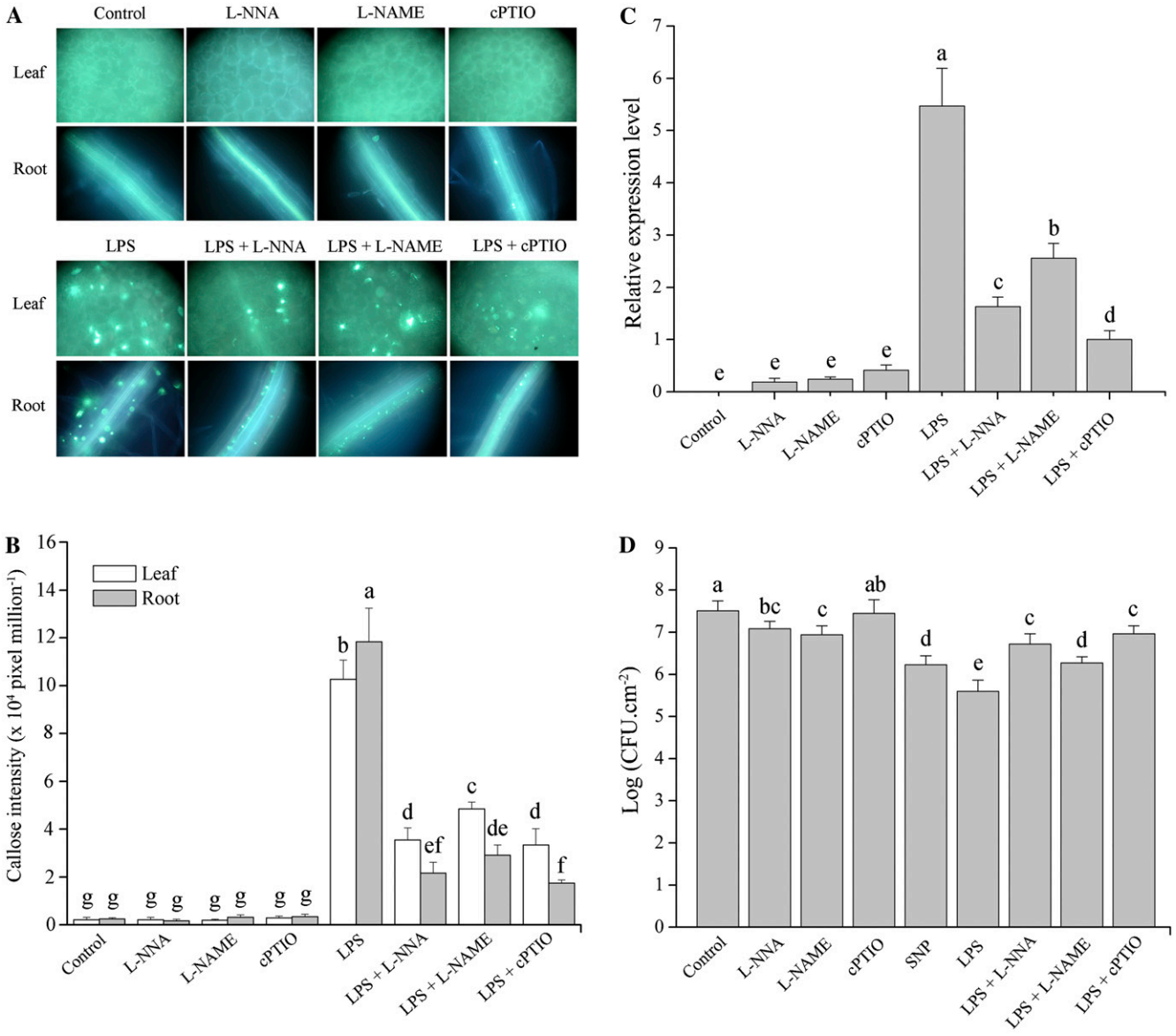

Figure 8. Effects of NO scavenger and mammalian NOS inhibitors on LPS-induced defense response. A, Effects of mammalian NOS inhibitors and NO scavenger on callose deposition. B, Callose deposition in leaves and roots was quantified by determining the number of pixels (corresponding to LPS-induced callose) per million pixels in digital photographs. Data are means ± SE of three experiments. C, *PR1* expression in leaves treated with control solution, 100 μg mL^{-1} LPS, 100 μg mL^{-1} LPS + 300 μM L-NNA, 100 μg mL^{-1} LPS + 300 μM L-NAME, or 100 μg mL^{-1} LPS + 1 mM cPTIO. Samples were harvested at 12 h post treatment for quantitative RT-PCR analysis. Arabidopsis *ACTIN2* was used as an internal control. Expression levels for each treatment were normalized to plants treated with LPS + cPTIO. Each value is the mean ± SE of three independent experiments. D, Bacterial growth quantification of *Pma* DG3-inoculated (OD_{600} = 0.0001) leaves after various treatments for 12 h. Samples were collected at 3 dpi for assay. Each value is the mean ± SE of three replicates. Different letters indicate statistically significant differences between treatments (Duncan's multiple range test: $P < 0.05$). CFU, Colony-forming units. [See online article for color version of this figure.]

of the GSH redox state and antioxidant capacity further supported that LPS-elicited NO generation as well as increased antioxidant enzyme activities capable of maintaining the redox state could be important to protect plants against oxidative damage from *Pma* DG3 attack (Figs. 5–7). We also found that inhibitors of mammalian NOS, together with LPS treatment, partially inhibited the LPS-induced effect (Fig. 8). Exogenous application of the NO donor SNP could decrease the development of disease. These findings confirm the significant contribution of NO to LPS-induced resistance responses in plants.

LPS-Induced Defense Responses Are Dependent on NPR1

NPR1 plays an important role in defense gene activation (Zhang et al., 1999; Ahn et al., 2007). During pathogen or SA induction, NPR1 regulates the high transcript accumulation of the callose synthase genes *CalS1* and *CalS12* (Dong et al., 2008). However, little is known about the signal transduction pathway leading to LPS-triggered defense responses. The LPS-induced increases in both *PR1* transcripts and callose deposition were nullified in *npr1* mutant plants (Fig. 3, B and C), and these effects were correlated with a faster development of disease lesions in *npr1* plants (Fig. 1). These findings highlight the importance of NPR1 in LPS-induced immune responses. NO is a redox regulator of the NPR1/TGA1 system that promotes the nuclear translocation of NPR1 (Lindermayr et al., 2010). We found that NPR1-dependent *PR1* expression and callose deposition induced by LPS were impaired by inhibitors of mammalian NOS and NO scavenger (Fig. 8, A–C); this result points to the involvement of NO in regulating NPR1-dependent responses. On the other hand, the NO-mediated up-regulation of SOD, POD, and CAT activities, as well as *AOX1a/b* expression, was affected in the *npr1* mutant (Figs. 5F and 6D). It is likely that NPR1 and NO act somewhat synergistically in mediating LPS-triggered defense responses. Further studies are needed to elucidate this mechanism. Nuclear localization of NPR1 is required for SA signal transduction to activate *PR* gene expression upon SAR induction (Kinkema et al., 2000). In a non-induced state, oxidized NPR1 forms an inactive oligomeric complex that remains in the cytosol; meanwhile, intermolecular disulfide bonds of NPR1 are reduced under SAR induction, thus leading to the translocation of NPR1 to the nucleus (Mou et al., 2003; Pieterse and Van Loon, 2004). We observed enhanced nuclear fluorescence of NPR1-GFP in guard cells after LPS induction (Fig. 4). Although more recent studies argue that the isochorismate synthase-mediated pathway is the predominant route for pathogen-induced SA accumulation in Arabidopsis, plant enzymes that convert isochorismate to SA have not been identified; other evidence suggest that a Phe ammonia lyase-mediated pathway also is operational in disease resistance (Dempsey et al., 2011). We found that AIP-mediated inhibition of Phe ammonia lyase partially, but not fully, suppressed the nuclear localization of NPR1 induced by LPS. The nuclear localization of NPR1 after LPS treatment suggests that SA-linked NPR1 signal pathways are mechanistically involved in LPS-activated defense progress.

CONCLUSION

Our investigations provide evidence that NO is responsible for NPR1-dependent innate immunity in plants by LPS. The possible signaling pathways for LPS-induced plant innate immunity are summarized in the model presented in Figure 9: LPS induce the Arg-utilizing source of NO production and nuclear localization of NPR1; NO, in turn, up-regulates antioxidant enzyme activity and/or promotes the nuclear translocation of NPR1 to induce *PR1* expression and callose deposition. The directly induced *PR1* expression

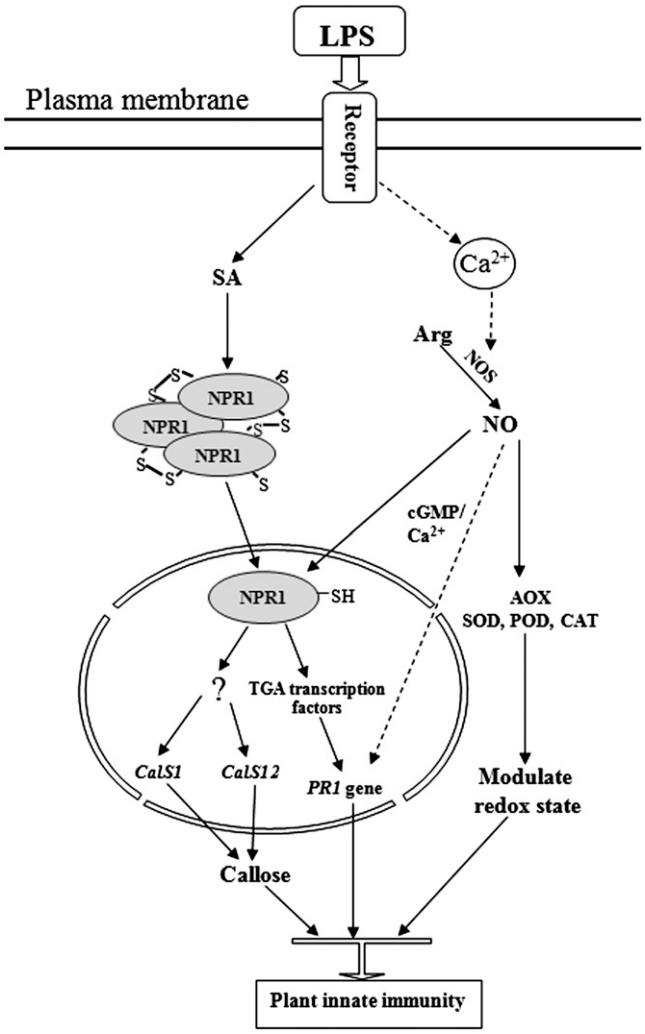

Figure 9. Model showing the possible signaling pathway for LPS-induced plant innate immunity. The extracellular LPS are recognized by a receptor in the plant cell plasma membrane. LPS perceived by receptors result in an increase in cytosolic Ca^{2+} (Ali et al., 2007; Ma et al., 2009), which may activate NOS-like enzyme and then lead to an increase of NO level. NO functions to potentiate cyclic GMP/Ca^{2+}-dependent *PR1* gene expression (Durner et al., 1998) as well as up-regulation of antioxidant enzyme activity, and/or promote the nuclear translocation of NPR1 to induce *PR1* expression (Lindermayr et al., 2010). LPS perception is mechanistically linked to NPR1-dependent defense responses. Induction by LPS results in the accumulation of SA and the activation of NPR1. Activated NPR1 then translocates into the nucleus, where it may interact with TGA transcription factors, thus leading to the induction of the *PR1* gene, and it also activates the expression of *CalS1* and *CalS12* genes in the formation of callose by interacting with some unknown transcription factors. These directly induced *PR1* expression and callose deposition by LPS constitute plant innate immunity, which protects plants against pathogen infection.

and callose deposition by LPS constitute plant innate immunity, which protects plants against pathogen infection. Our results contribute to the elucidation of the signaling mechanism of NO, and they highlight an important role of NPR1 in modulating LPS-triggered innate immunity in plants.

MATERIALS AND METHODS

Plant Material and Chemicals

Seeds of wild-type (ecotype Columbia) Arabidopsis (*Arabidopsis thaliana*), *npr1*, *Atnoa1*, *nia1nia2*, *cue1*, and *gsnor1-3* plants, transgenic mit-roGFP1, *PR1*:*GUS* transgenic Arabidopsis, and the transgenic *35S*::*NPR1-GFP* in *npr1* mutant Arabidopsis (Kinkema et al., 2000) were sterilized and grown in soil or grown on solid MS medium as described previously (Zhang and Xing, 2008).

3-Amino,4-aminomethyl-2′,7′-difluorescein diacetate (DAF-FM DA) and cPTIO were obtained from Molecular Probes. LPS, SNP, SHAM, sodium tungstate, L-Arg, L-NNA, L-NAME, 5-bromo-4-chloro-3-indolyl-β-D-glucuronide, and diethyldithiocarbamate (DETC) were purchased from Sigma-Aldrich. Aniline blue was purchased from Acros Organics.

LPS Preparation and Treatment

LPS were purchased from Sigma-Aldrich and dissolved as described previously (Zeidler et al., 2004). For all experiments, the work concentration of LPS was 100 μg mL^{-1} based on previous studies (Melotto et al., 2006). To treat protoplasts, 100 μg mL^{-1} LPS was added to protoplast suspension on 48-well plates and incubated for the indicated time period at room temperature.

Pathogen Growth and Inoculation

The bacterial strain used in this study was *Pseudomonas syringae* pv *maculicola* (*Pma*) DG3, and it was grown at 28°C in King's B medium supplemented with appropriate antibiotics (Lu et al., 2003). Overnight log-phase cultures were collected by centrifugation, washed with 10 mM $MgCl_2$, and then diluted to a final optical density at 600 nm (OD_{600}) of 0.01 (for appearance determination) and 0.0001 (for pathogen growth assay). The procedures of pathogen inoculation and bacteria growth assays were as described previously (Mishina and Zeier, 2007).

Protoplast Isolation

Protoplast isolation was performed using 14- to 21-d-old Arabidopsis according to a procedure described previously (He et al., 2007; Li et al., 2012). The purified protoplasts were washed three times with W5 solution (154 mM NaCl, 125 mM $CaCl_2$, 5 mM KCl, 5 mM Glc, and 1.5 mM MES-KOH, pH 5.6) and adjusted to a density between 10^5 and 10^6 protoplasts mL^{-1} with W5 solution.

NO Labeling and Measurements

The Arabidopsis protoplasts loaded with DAF-FM DA were analyzed as described previously (Yao and Greenberg, 2006). Briefly, freshly isolated protoplasts on 48-well cell culture plates were preloaded with DAF-FM DA at room temperature. Subsequently, protoplasts were washed three times with W5 solution before treatment. Microscopic observations were performed by a Zeiss LSM510 laser confocal scanning microscope. DAF-FM and GFP signals were visualized by using an excitation wavelength of 488 nm and a bandpass 500- to 550-nm filter. The fluorescence intensity of DAF-FM was also detected with an LS 55 Luminescence Spectrophotometer (Perkin-Elmer) with an excitation wavelength of 488 nm and emission wavelengths between 500 and 550 nm (Ye et al., 2012). The fluorescence intensity at 515 nm was used to determine the relative NO generation.

NO Detection by EPR

After 2 h of treatment, 500 μL of cells was harvested and then were incubated in 0.6 mL of buffered solution (50 mM HEPES, 1 mM dithiothreitol, and 1 mM $MgCl_2$, pH 7.6) at 37°C for 2 min. After sample preparation, the supernatant was added to 300 μL of freshly made Fe(II)$(DETC)_2$ solution (2 M $Na_2S_2O_4$, 3.3 mM DETC, 3.3 mM $FeSO_4$, and 33 g L^{-1} bovine serum albumin) and analyzed with a Bruker A200 spectrometer (Bruker Instrument) under the following conditions: microwave frequency, 9.86 GHz; microwave power, 19 mW; modulation frequency, 100 kHz.

Histochemical GUS Staining

Approximately 10-d-old transgenic *PR1*:*GUS* seedlings grown on MS medium were transferred to 24-well plates containing 400 μL of liquid MS medium with or without 100 μg mL^{-1} LPS at the indicated times. Histochemical detection of GUS enzyme activity was performed as described previously (Gust et al., 2007). After staining with 0.5 mg mL^{-1} 5-bromo-4-chloro-3-indolyl-β-D-glucuronide solution, the samples were boiled in 95% ethanol for 10 min to remove the chlorophyll.

Callose Staining

Approximately 10-d-old seedlings grown on MS medium were transferred to 24-well plates containing 400 μL of liquid MS medium with 100 μg mL^{-1} LPS and/or other solutions for 24 h. The leaves and roots from wild-type or *npr1* plants were fixed in ethanol:acetic acid (3:1, v/v) and stained with 0.01% (w/v) aniline blue (Millet et al., 2010). The leaves or roots were mounted on slides, and callose was observed with UV excitation.

Visualization of NPR1

Ten-day-old seedlings expressing NPR1-GFP grown on MS medium were transferred to 24-well plates containing 400 μL of liquid MS medium with 100 μg mL^{-1} LPS and/or other solutions and then were analyzed for GFP fluorescence after 12-h treatments. Arabidopsis leaf tissues were mounted in water and imaged with a Zeiss LSM510 for guard cell assays. GFP fluorescence was captured following excitation at 488 nm and detection at 505 to 550 nm.

RNA Extraction and RT-PCR Analysis

Total RNA was extracted using the TRIzol reagent (Invitrogen) according to the manufacturer's specifications. First-strand complementary DNA was synthesized from total RNA using a Reverse-iT first-strand synthesis kit (ABgene).

The transcript levels of *CalS1* and *CalS12* genes were analyzed by gel analysis and were quantified from the gel photographs. The gene-specific primers of *CalS1* and *CalS12* were used as described (Dong et al., 2008). The *ACTIN2* gene was amplified as a semiquantitative control (Fan et al., 2008).

The transcripts of *AOX* genes, *PR1*, *NIA1*, and *NIA2* were analyzed by quantitative RT-PCR. The gene-specific primers were used as described (Umbach et al., 2005; Mang et al., 2009; Konishi and Yanagisawa, 2011). The *ACTIN2* gene was amplified as a quantitative control (Fan et al., 2008). For quantitative RT-PCR analyses, the Light Cycler 2.0 instrument (Roche Applied Science) and SYBR Green real-time PCR master mix (Toyobo) were used to run the three-step program. PCR cycling conditions for amplification were 95°C for 60 s followed by 40 cycles of 95°C for 5 s, 55°C for 10 s, and 72°C for 30 s. Relative expression levels were calculated using the $2^{(-\Delta\Delta Ct)}$ analysis method (Livak and Schmittgen, 2001).

Enzyme Activity Assays

NOS activity was determined with the NOS Assay Kit (Sigma). Freshly isolated protoplasts were incubated with LPS or in the presence of mammalian NOS inhibitors and were measured according to the manufacturer's instructions. The fluorescent product, which was formed from 4,5-diaminofluorescein reacted with NO produced by NOS, was measured using an excitation filter at 492 nm and an emission filter at 515 nm. The activity of NOS was expressed as a relative value.

The NR activity was determined following the modified method (Zhao et al., 2009). The activities of three antioxidant enzymes, CAT, POD, and SOD, were spectrophotometrically measured as described previously (Huang et al., 2010). SOD activity was detected by monitoring the absorbance decrease at 560 nm due to the inhibition of nitroblue tetrazolium reduction. One unit of SOD activity was defined as the amount of enzyme that inhibits the photochemical reduction of nitroblue tetrazolium to 50%, considering the absorbance of the

control mixture as 100%. The increase in A_{470} was measured for POD activity, and one unit of POD activity was defined as the increase of absorbance by 0.01 per min. The CAT activity was determined at 240 nm, and one unit of CAT activity was defined as the decrease of absorbance by 0.01 per min.

DAB Staining

For H_2O_2 detection, healthy or infected leaves were incubated in 1 mg mL^{-1} DAB solution (1 mg mL^{-1}; pH 5.5) in the dark for 8 h (Liu et al., 2007). The leaves were then cleared by boiling in 95% ethanol for 10 min to remove the chlorophyll completely. The reddish color of the leaves as evidence of H_2O_2 was visualized by light microscopy. For each treatment, the percentage of stained DAB area was determined by the software ImageJ.

Measurements of roGFP1 Fluorescence

The roGFP1 degree of oxidation was determined as described (Rosenwasser et al., 2010). Leaf discs were excited by using 400- ± 15-nm and 485- ± 10-nm filters, and fluorescence values were measured using a 525- ± 10-nm emission filter. Leaf pieces were perfused with 10 mM H_2O_2 and then 10 mM dithiothreitol to drive the roGFP1 toward the fully oxidized and reduced forms, respectively. The degree of oxidation of roGFP1 was calculated according to Schwarzländer et al. (2008).

Total Antioxidant Capacity

Total antioxidant capacity was detected by a total antioxidant capacity assay kit with the 2,2′-azino-bis(3-ethylbenzthiazoline-6-sulfonic acid) method (Beyotime). Measurements were performed in triplicate for each extract according to the manufacturer's specifications. Antioxidant capacity was determined relative to the reactivity of Trolox (6-hydroxy-2,5,7,8-tetramethylchroman-2-carboxylic acid) as a standard.

Determination of Glutathione

Glutathione levels were measured based on the 5,5′-dithiobis(2-nitrobenzoic acid)-recycling enzymatic method. The extracted samples were divided in half for assay of total glutathione (GSH + GSSG) and for GSSG alone as described previously (Ge et al., 2007). The absorbance change at 412 nm was measured, and the glutathione concentration was evaluated by comparison with a standard calibration curve.

Sequence data from this article can be found in the GenBank/EMBL data libraries under accession numbers NM_100436 (*CalS1*), NM_116593 (*CalS12*), NM_106425 (*NIA1*), NM_103364 (*NIA2*), NM_113135 (*AOX1a*), NM_113134 (*AOX1b*), NM_113678 (*AOX1c*), NM_102968 (*AOX1d*), NM_125817 (*AOX2*), NM_127025 (*PR1*), and NM_112764 (*Actin2*).

Supplemental Data

The following materials are available in the online version of this article.

Supplemental Figure S1. Generation of NO under LPS induction in wild-type Arabidopsis protoplasts.

Supplemental Figure S2. Induction of *PR1* gene expression and callose deposition in fully grown Arabidopsis by LPS.

Supplemental Figure S3. Generation of NO in guard cells of wild-type plants during LPS induction.

Supplemental Figure S4. Effect of 1 mM cPTIO on protoplast viability.

Supplemental Figure S5. LPS-induced nuclear localization of NPR1 in protoplasts.

Supplemental Figure S6. The changes of fluorescence intensity and the resulting ratios in transgenic mit-roGFP1 plants.

Supplemental Figure S7. Quantitative RT-PCR analysis of *NIA1* and *NIA2* transcriptions under LPS induction in wild-type plants.

ACKNOWLEDGMENTS

We thank Dr. Wenhao Zhang, Dr. Andrea A. Gust, and Dr. Xinnian Dong for kindly providing seeds of *nia1nia2* plants, *PR1:GUS* transgenic Arabidopsis, and transgenic *35S::NPR1-GFP* in the *npr1* mutant Arabidopsis. We also thank Lingrui Zhang and Zhe Li for their constructive discussions.

Received June 11, 2012; accepted August 26, 2012; published August 27, 2012.

LITERATURE CITED

Ahn IP, Kim S, Lee YH, Suh SC (2007) Vitamin B1-induced priming is dependent on hydrogen peroxide and the *NPR1* gene in Arabidopsis. Plant Physiol **143:** 838–848

Ali R, Ma W, Lemtiri-Chlieh F, Tsaltas D, Leng Q, von Bodman S, Berkowitz GA (2007) Death don't have no mercy and neither does calcium: *Arabidopsis* CYCLIC NUCLEOTIDE GATED CHANNEL2 and innate immunity. Plant Cell **19:** 1081–1095

Apel K, Hirt H (2004) Reactive oxygen species: metabolism, oxidative stress, and signal transduction. Annu Rev Plant Biol **55:** 373–399

Besson-Bard A, Pugin A, Wendehenne D (2008) New insights into nitric oxide signaling in plants. Annu Rev Plant Biol **59:** 21–39

Bethke PC, Badger MR, Jones RL (2004) Apoplastic synthesis of nitric oxide by plant tissues. Plant Cell **16:** 332–341

Braun SG, Meyer A, Holst O, Pühler A, Niehaus K (2005) Characterization of the *Xanthomonas campestris* pv. *campestris* lipopolysaccharide substructures essential for elicitation of an oxidative burst in tobacco cells. Mol Plant Microbe Interact **18:** 674–681

Cohn J, Sessa G, Martin GB (2001) Innate immunity in plants. Curr Opin Immunol **13:** 55–62

Corpas FJ, Barroso JB, Carreras A, Quirós M, León AM, Romero-Puertas MC, Esteban FJ, Valderrama R, Palma JM, Sandalio LM, et al (2004) Cellular and subcellular localization of endogenous nitric oxide in young and senescent pea plants. Plant Physiol **136:** 2722–2733

Corpas FJ, Leterrier M, Valderrama R, Airaki M, Chaki M, Palma JM, Barroso JB (2011) Nitric oxide imbalance provokes a nitrosative response in plants under abiotic stress. Plant Sci **181:** 604–611

Corpas FJ, Palma JM, del Río LA, Barroso JB (2009) Evidence supporting the existence of L-arginine-dependent nitric oxide synthase activity in plants. New Phytol **184:** 9–14

Crawford NM, Galli M, Tischner R, Heimer YM, Okamoto M, Mack A (2006) Response to Zemojtel et al.: Plant nitric oxide synthase: back to square one. Trends Plant Sci **11:** 526–527

Delledonne M (2005) NO news is good news for plants. Curr Opin Plant Biol **8:** 390–396

Delledonne M, Xia Y, Dixon RA, Lamb C (1998) Nitric oxide functions as a signal in plant disease resistance. Nature **394:** 585–588

Dempsey DA, Vlot AC, Wildermuth MC, Klessig DF (2011) Salicylic acid biosynthesis and metabolism. The Arabidopsis Book **9:** e0156, doi/10.1199/tab.0156

Desaki Y, Miya A, Venkatesh B, Tsuyumu S, Yamane H, Kaku H, Minami E, Shibuya N (2006) Bacterial lipopolysaccharides induce defense responses associated with programmed cell death in rice cells. Plant Cell Physiol **47:** 1530–1540

Dong X, Hong Z, Chatterjee J, Kim S, Verma DPS (2008) Expression of callose synthase genes and its connection with *Npr1* signaling pathway during pathogen infection. Planta **229:** 87–98

Dow M, Newman MA, von Roepenack E (2000) The induction and modulation of plant defense responses by bacterial lipopolysaccharides. Annu Rev Phytopathol **38:** 241–261

Durner J, Wendehenne D, Klessig DF (1998) Defense gene induction in tobacco by nitric oxide, cyclic GMP, and cyclic ADP-ribose. Proc Natl Acad Sci USA **95:** 10328–10333

Fan LM, Zhang W, Chen JG, Taylor JP, Jones AM, Assmann SM (2008) Abscisic acid regulation of guard-cell K^+ and anion channels in Gβ- and RGS-deficient Arabidopsis lines. Proc Natl Acad Sci USA **105:** 8476–8481

Feechan A, Kwon E, Yun BW, Wang Y, Pallas JA, Loake GJ (2005) A central role for *S*-nitrosothiols in plant disease resistance. Proc Natl Acad Sci USA **102:** 8054–8059

Fröhlich A, Durner J (2011) The hunt for plant nitric oxide synthase (NOS): is one really needed? Plant Sci **181:** 401–404

Fu LJ, Shi K, Gu M, Zhou YH, Dong DK, Liang WS, Song FM, Yu JQ (2010) Systemic induction and role of mitochondrial alternative oxidase and nitric oxide in a compatible tomato-*Tobacco mosaic virus* interaction. Mol Plant Microbe Interact **23:** 39–48

Galletti R, Denoux C, Gambetta S, Dewdney J, Ausubel FM, De Lorenzo G, Ferrari S (2008) The AtrbohD-mediated oxidative burst elicited by oligogalacturonides in Arabidopsis is dispensable for the activation of defense responses effective against *Botrytis cinerea*. Plant Physiol **148:** 1695–1706

Ge X, Li GJ, Wang SB, Zhu H, Zhu T, Wang X, Xia Y (2007) AtNUDT7, a negative regulator of basal immunity in Arabidopsis, modulates two distinct defense response pathways and is involved in maintaining redox homeostasis. Plant Physiol **145:** 204–215

Gómez-Gómez L, Felix G, Boller T (1999) A single locus determines sensitivity to bacterial flagellin in *Arabidopsis thaliana*. Plant J **18:** 277–284

Guo FQ, Okamoto M, Crawford NM (2003) Identification of a plant nitric oxide synthase gene involved in hormonal signaling. Science **302:** 100–103

Gupta KJ, Fernie AR, Kaiser WM, van Dongen JT (2011) On the origins of nitric oxide. Trends Plant Sci **16:** 160–168

Gust AA, Biswas R, Lenz HD, Rauhut T, Ranf S, Kemmerling B, Götz F, Glawischnig E, Lee J, Felix G, et al (2007) Bacteria-derived peptidoglycans constitute pathogen-associated molecular patterns triggering innate immunity in Arabidopsis. J Biol Chem **282:** 32338–32348

He P, Shan L, Sheen J (2007) The use of protoplasts to study innate immune responses. Methods Mol Biol **354:** 1–9

Huang XS, Liu JH, Chen XJ (2010) Overexpression of *PtrABF* gene, a bZIP transcription factor isolated from *Poncirus trifoliata*, enhances dehydration and drought tolerance in tobacco via scavenging ROS and modulating expression of stress-responsive genes. BMC Plant Biol **10:** 230–247

Jasid S, Simontacchi M, Bartoli CG, Puntarulo S (2006) Chloroplasts as a nitric oxide cellular source: effect of reactive nitrogen species on chloroplastic lipids and proteins. Plant Physiol **142:** 1246–1255

Jones JD, Dangl JL (2006) The plant immune system. Nature **444:** 323–329

Kinkema M, Fan W, Dong X (2000) Nuclear localization of NPR1 is required for activation of PR gene expression. Plant Cell **12:** 2339–2350

Konishi M, Yanagisawa S (2011) The regulatory region controlling the nitrate-responsive expression of a nitrate reductase gene, *NIA1*, in Arabidopsis. Plant Cell Physiol **52:** 824–836

Lee U, Wie C, Fernandez BO, Feelisch M, Vierling E (2008) Modulation of nitrosative stress by S-nitrosoglutathione reductase is critical for thermotolerance and plant growth in *Arabidopsis*. Plant Cell **20:** 786–802

Li Z, Yue H, Xing D (2012) MAP kinase 6-mediated activation of vacuolar processing enzyme modulates heat shock-induced programmed cell death in Arabidopsis. New Phytol **195:** 85–96

Lillo C, Meyer C, Lea US, Provan F, Oltedal S (2004) Mechanism and importance of post-translational regulation of nitrate reductase. J Exp Bot **55:** 1275–1282

Lindermayr C, Sell S, Müller B, Leister D, Durner J (2010) Redox regulation of the NPR1-TGA1 system of *Arabidopsis thaliana* by nitric oxide. Plant Cell **22:** 2894–2907

Liu Y, Ren D, Pike S, Pallardy S, Gassmann W, Zhang S (2007) Chloroplast-generated reactive oxygen species are involved in hypersensitive response-like cell death mediated by a mitogen-activated protein kinase cascade. Plant J **51:** 941–954

Livak KJ, Schmittgen TD (2001) Analysis of relative gene expression data using real-time quantitative PCR and the $2^{-\Delta\Delta C_T}$ method. Methods **25:** 402–408

Lu H, Rate DN, Song JT, Greenberg JT (2003) ACD6, a novel ankyrin protein, is a regulator and an effector of salicylic acid signaling in the *Arabidopsis* defense response. Plant Cell **15:** 2408–2420

Ma W, Qi Z, Smigel A, Walker RK, Verma R, Berkowitz GA (2009) Ca^{2+}, cAMP, and transduction of non-self perception during plant immune responses. Proc Natl Acad Sci USA **106:** 20995–21000

Mang HG, Laluk KA, Parsons EP, Kosma DK, Cooper BR, Park HC, AbuQamar S, Boccongelli C, Miyazaki S, Consiglio F, et al (2009) The Arabidopsis *RESURRECTION1* gene regulates a novel antagonistic interaction in plant defense to biotrophs and necrotrophs. Plant Physiol **151:** 290–305

Melotto M, Underwood W, Koczan J, Nomura K, He SY (2006) Plant stomata function in innate immunity against bacterial invasion. Cell **126:** 969–980

Millet YA, Danna CH, Clay NK, Songnuan W, Simon MD, Werck-Reichhart D, Ausubel FM (2010) Innate immune responses activated in *Arabidopsis* roots by microbe-associated molecular patterns. Plant Cell **22:** 973–990

Mishina TE, Zeier J (2007) Pathogen-associated molecular pattern recognition rather than development of tissue necrosis contributes to bacterial induction of systemic acquired resistance in Arabidopsis. Plant J **50:** 500–513

Mittler R (2002) Oxidative stress, antioxidants and stress tolerance. Trends Plant Sci **7:** 405–410

Moore AL, Albury MS, Crichton PG, Affourtit C (2002) Function of the alternative oxidase: is it still a scavenger? Trends Plant Sci **7:** 478–481

Moreau M, Lee GI, Wang Y, Crane BR, Klessig DF (2008) AtNOS/AtNOA1 is a functional *Arabidopsis thaliana* cGTPase and not a nitric-oxide synthase. J Biol Chem **283:** 32957–32967

Mou Z, Fan W, Dong X (2003) Inducers of plant systemic acquired resistance regulate NPR1 function through redox changes. Cell **113:** 935–944

Mur LA, Mandon J, Cristescu SM, Harren FJ, Prats E (2011) Methods of nitric oxide detection in plants: a commentary. Plant Sci **181:** 509–519

Neill S, Bright J, Desikan R, Hancock J, Harrison J, Wilson I (2008) Nitric oxide evolution and perception. J Exp Bot **59:** 25–35

Newman MA, von Roepenack-Lahaye E, Parr A, Daniels MJ, Dow JM (2002) Prior exposure to lipopolysaccharide potentiates expression of plant defenses in response to bacteria. Plant J **29:** 487–495

Nürnberger T, Brunner F, Kemmerling B, Piater L (2004) Innate immunity in plants and animals: striking similarities and obvious differences. Immunol Rev **198:** 249–266

Palmieri MC, Lindermayr C, Bauwe H, Steinhauser C, Durner J (2010) Regulation of plant glycine decarboxylase by *S*-nitrosylation and glutathionylation. Plant Physiol **152:** 1514–1528

Peterson DA, Peterson DC, Archer S, Weir EK (1992) The non specificity of specific nitric oxide synthase inhibitors. Biochem Biophys Res Commun **187:** 797–801

Pieterse CM, Van Loon LC (2004) NPR1: the spider in the web of induced resistance signaling pathways. Curr Opin Plant Biol **7:** 456–464

Rasul S, Dubreuil-Maurizi C, Lamotte O, Koen E, Poinssot B, Alcaraz G, Wendehenne D, Jeandroz S (2012) Nitric oxide production mediates oligogalacturonide-triggered immunity and resistance to *Botrytis cinerea* in *Arabidopsis thaliana*. Plant Cell Environ **35:** 1483–1499

Rockel P, Strube F, Rockel A, Wildt J, Kaiser WM (2002) Regulation of nitric oxide (NO) production by plant nitrate reductase *in vivo* and *in vitro*. J Exp Bot **53:** 103–110

Rosenwasser S, Rot I, Meyer AJ, Feldman L, Jiang K, Friedman H (2010) A fluorometer-based method for monitoring oxidation of redox-sensitive GFP (roGFP) during development and extended dark stress. Physiol Plant **138:** 493–502

Scheel D (1998) Resistance response physiology and signal transduction. Curr Opin Plant Biol **1:** 305–310

Schwarzländer M, Fricker MD, Müller C, Marty L, Brach T, Novak J, Sweetlove LJ, Hell R, Meyer AJ (2008) Confocal imaging of glutathione redox potential in living plant cells. J Microsc **231:** 299–316

Tena G, Asai T, Chiu WL, Sheen J (2001) Plant mitogen-activated protein kinase signaling cascades. Curr Opin Plant Biol **4:** 392–400

Ton J, Mauch-Mani B (2004) β-Amino-butyric acid-induced resistance against necrotrophic pathogens is based on ABA-dependent priming for callose. Plant J **38:** 119–130

Umbach AL, Fiorani F, Siedow JN (2005) Characterization of transformed Arabidopsis with altered alternative oxidase levels and analysis of effects on reactive oxygen species in tissue. Plant Physiol **139:** 1806–1820

van Hulten M, Pelser M, van Loon LC, Pieterse CMJ, Ton J (2006) Costs and benefits of priming for defense in *Arabidopsis*. Proc Natl Acad Sci USA **103:** 5602–5607

van Loon LC, van Strein EA (1999) The families of pathogenesis-related proteins, their activities, and comparative analysis of PR-1 type proteins. Physiol Mol Plant Pathol **55:** 85–97

Van Ree K, Gehl B, Chehab EW, Tsai YC, Braam J (2011) Nitric oxide accumulation in Arabidopsis is independent of NOA1 in the presence of sucrose. Plant J **68:** 225–233

Wimalasekera R, Villar C, Begum T, Scherer GF (2011) COPPER AMINE OXIDASE1 (CuAO1) of Arabidopsis thaliana contributes to abscisic

acid- and polyamine-induced nitric oxide biosynthesis and abscisic acid signal transduction. Mol Plant **4:** 663–678

Yao N, Greenberg JT (2006) *Arabidopsis* ACCELERATED CELL DEATH2 modulates programmed cell death. Plant Cell **18:** 397–411

Ye Y, Li Z, Xing D (2012) Nitric oxide promotes MPK6-mediated caspase-3-like activation in cadmium-induced Arabidopsis thaliana programmed cell death. Plant Cell Environ (in press)

Zeidler D, Zähringer U, Gerber I, Dubery I, Hartung T, Bors W, Hutzler P, Durner J (2004) Innate immunity in *Arabidopsis thaliana*: lipopolysaccharides activate nitric oxide synthase (NOS) and induce defense genes. Proc Natl Acad Sci USA **101:** 15811–15816

Zemojtel T, Fröhlich A, Palmieri MC, Kolanczyk M, Mikula I, Wyrwicz LS, Wanker EE, Mundlos S, Vingron M, Martasek P, et al (2006) Plant nitric oxide synthase: a never-ending story? Trends Plant Sci **11:** 524–525, author reply 526–528

Zhang LR, Xing D (2008) Methyl jasmonate induces production of reactive oxygen species and alterations in mitochondrial dynamics that precede photosynthetic dysfunction and subsequent cell death. Plant Cell Physiol **49:** 1092–1111

Zhang Y, Fan W, Kinkema M, Li X, Dong X (1999) Interaction of NPR1 with basic leucine zipper protein transcription factors that bind sequences required for salicylic acid induction of the *PR-1* gene. Proc Natl Acad Sci USA **96:** 6523–6528

Zhao MG, Chen L, Zhang LL, Zhang WH (2009) Nitric reductase-dependent nitric oxide production is involved in cold acclimation and freezing tolerance in Arabidopsis. Plant Physiol **151:** 755–767